



Deposited via The University of Sheffield.

White Rose Research Online URL for this paper:

<https://eprints.whiterose.ac.uk/id/eprint/162403/>

Version: Accepted Version

Article:

Gibson, J.F., Prajsnar, T.K., Hill, C.J. et al. (2021) Neutrophils use selective autophagy receptor Sqstm1/p62 to target Staphylococcus aureus for degradation in vivo in zebrafish. *Autophagy*, 17 (6). pp. 1448-1457. ISSN: 1554-8627

<https://doi.org/10.1080/15548627.2020.1765521>

This is an Accepted Manuscript of an article published by Taylor & Francis in *Autophagy* on 19 Jun 2020, available online:

<http://www.tandfonline.com/10.1080/15548627.2020.1765521>.

Reuse

Items deposited in White Rose Research Online are protected by copyright, with all rights reserved unless indicated otherwise. They may be downloaded and/or printed for private study, or other acts as permitted by national copyright laws. The publisher or other rights holders may allow further reproduction and re-use of the full text version. This is indicated by the licence information on the White Rose Research Online record for the item.

Takedown

If you consider content in White Rose Research Online to be in breach of UK law, please notify us by emailing eprints@whiterose.ac.uk including the URL of the record and the reason for the withdrawal request.

1 **Neutrophils use selective autophagy receptor Sqstm1/p62 to target**
2 ***Staphylococcus aureus* for degradation *in vivo* in zebrafish**

3
4 Josie F Gibson^{1,2,3,4,5}, Tomasz K Prajsnar^{1,2,6}, Christopher J Hill⁵, Amy K Tooke⁵, Justyna J
5 Serba^{1,2}, Rebecca D Tonge⁷, Simon J Foster^{4,5}, Andrew J Grierson^{2,7}, Philip W Ingham^{3,8#},
6 Stephen A Renshaw^{1,2,4#}, Simon A Johnston^{1,2,4#}.

- 7
8
9
10
11 1. Department of Infection, Immunity and Cardiovascular disease, Medical School, University of Sheffield, S10 2RX UK.
12 2. The Bateson Centre, University of Sheffield, Sheffield, S10 2TN, UK
13 3. Institute of Molecular and Cell Biology, Agency of Science, Technology and Research (A-Star), Singapore 138673
14 4. Florey Institute, University of Sheffield, Sheffield, United Kingdom, S10 2TN
15 5. Department of Molecular Biology and Biotechnology, University of Sheffield, S10 2TN, UK
16 6. Institute Biology Leiden, Leiden University, Leiden, The Netherlands
17 7. Sheffield institute for Translational Neuroscience, Department of Neuroscience, University of Sheffield, S10 2HQ, UK
18 8. Lee Kong Chian School of Medicine, Nanyang Technological University, Singapore 636921

19
20 *Correspondence: s.a.johnston@sheffield.ac.uk
21 #Joint senior author
22
23
24
25
26
27
28
29
30
31
32
33
34
35
36
37
38
39
40
41
42
43
44
45
46

47 **Keywords:** autophagy, bacterial infection, host-pathogen interactions, neutrophil,
48 *staphylococcus aureus*, SQSTM1/p62, xenophagy, zebrafish.
49
50
51
52
53
54
55
56
57

58 **Abstract**

59
60 Macroautophagy/autophagy functions to degrade cellular components and intracellular
61 pathogens. Autophagy receptors, including SQSTM1/p62, target intracellular pathogens.
62 *Staphylococcus aureus* is a significant pathogen of humans, especially in
63 immunocompromise. *S. aureus* may use neutrophils as a proliferative niche, but their
64 intracellular fate following phagocytosis has not been analyzed *in vivo*. *In vitro*, SQSTM1 can
65 colocalize with intracellular *Staphylococcus aureus*, but whether SQSTM1 is beneficial or
66 detrimental in host defense against *S. aureus in vivo* is unknown. Here we determine the
67 fate and location of *S. aureus* within neutrophils throughout zebrafish infection. We show Lc3
68 and Sqstm1 recruitment to phagocytosed *S. aureus* is altered depending on the bacterial
69 location within the neutrophil and that Lc3 marking of bacterial phagosomes within
70 neutrophils may precede bacterial degradation. Finally, we show Sqstm1 is important for
71 controlling cytosolic bacteria, demonstrating for the first time a key role of Sqstm1 in
72 autophagic control of *S. aureus* in neutrophils.

73
74
75
76
77
78

79 **Abbreviations:** AR: autophagy receptor; CFU: colony-forming unit; CHT: caudal
80 hematopoietic tissue; GFP: green fluorescent protein; hpf: hours post-fertilization; hpi: hours
81 post-infection; LWT: london wild-type; lyz: lysozyme; Map1lc3/Lc3: microtubule-associated
82 protein 1 light chain 3; RFP: red fluorescent protein; Sqstm1/p62: sequestosome 1; Tg:
83 transgenic; TSA: tyramide signal amplification; UBD: ubiquitin binding domain.

84
85

86 **Introduction**

87

88 Autophagy (macroautophagy) is a process of cellular self-degradation, in which damaged or
89 redundant cellular components are taken into an autophagosome and subsequently
90 trafficked to the lysosome for degradation; these degraded components can then be
91 recycled for alternative uses by the cell [1,2]. During infection, autophagy is used by host
92 cells to degrade invading pathogens, a process termed xenophagy [3,4].

93

94 Autophagy is considered largely non-selective of the cargo to be degraded, classically being
95 induced by starvation conditions. However, selective autophagy is a process that enables
96 specific cargo to be directed into the autophagy pathway, which can be used to target
97 invading pathogens. Selective autophagy uses autophagy receptors (ARs), proteins that
98 interact with both autophagy machinery and the cargo to be degraded [5,6]. Many ARs are
99 involved in targeting invading pathogens, including SQSTM1/p62 (sequestosome 1), NBR1
100 (NBR1 autophagy cargo receptor), OPTN (optineurin) and CALCOCO2/NDP52 (calcium
101 binding and coiled-coil domain 2) [7].

102

103 Loss of autophagy function, for example, through mutations in key autophagy genes, can
104 increase the risk of infection with intracellular pathogens [8]. It is well established that
105 pathogen presence can induce host cell autophagy and that pathogens can be degraded by
106 this pathway. Intracellular pathogens such as *Mycobacterium marinum*, *Shigella flexneri* and
107 *Listeria monocytogenes* [9,10] can be targeted by ARs for degradation. Conversely,
108 pathogens have evolved to be able to block or subvert immune defenses, and autophagy is
109 no exception. Indeed, many bacterial pathogens are able to inhibit the induction of
110 autophagy or to reside within the autophagy pathway by preventing lysosomal fusion, or
111 even avoid making any contact with autophagic machinery [11]. In some cases, it is
112 beneficial to the pathogen to up-regulate the autophagy pathway, for example, *Legionella*
113 *pneumophila*, *Coxiella burnetii* and *Salmonella enterica* serovar typhimurium [12–14]. The
114 outcome of host-cell autophagy, therefore, differs between various invading pathogens.

115

116 *Staphylococcus aureus* is a bacterial pathogen that can reside within neutrophils as an
117 intracellular niche [15,16]. Autophagy has been implicated in *S. aureus* infection, but there
118 are conflicting reports suggesting autophagy might be either beneficial [17] or detrimental for
119 *S. aureus* [18]. Intracellular pathogens, including *S. aureus*, can escape the phagosome into
120 the cytosol [19], likely through toxins secreted by the bacteria or membrane rupture due to
121 bacterial growth. Once in the cytosol, bacteria can be ubiquitinated and targeted by ARs [7].
122 Indeed, Sqstm1 in fibroblasts and epithelial cells has been shown to localize to cytosolic S.

123 *aureus* leading to autophagosome formation *in vitro* [18,20]. Therefore, we investigated
124 whether Sqstm1 recruitment is employed by neutrophils in *S. aureus* infection and what
125 influence selective autophagy has on infection outcome *in vivo*.

126

127 In order to examine the role of neutrophil autophagy in *S. aureus* infection, we compared the
128 fate of bacterial cells following Map1lc3/Lc3 (microtubule-associated protein 1 light chain 3)
129 and Sqstm1 recruitment. We tested the role of Sqstm1 in pathogen handling *in vivo*, using
130 the genetic tractability of the zebrafish to create a neutrophil-specific Sqstm1-GFP
131 transgenic reporter and an *sqstm1* activity-deficient mutant. With this approach, we show
132 that Sqstm1 is recruited to cytosolic *S. aureus* and disruption of Sqstm1 expression or
133 function adversely affects *S. aureus* infection outcome.

134

135 **Results**

136

137 **Staphylococcus aureus location within neutrophils changes throughout infection.**

138

139 Autophagy responses have been demonstrated to change throughout the progression of the
140 infection. Targeting of pathogens by autophagy receptors is likely to occur at later time
141 points in infection. Therefore, to determine the fate and location of *S. aureus* in neutrophils
142 during infection, *S. aureus* expressing mCherry was inoculated and imaged at early (2 to 5 h
143 post-infection [hpi]) and late (24 to 28 hpi) time points. Initially, the well-established
144 *Tg(mpx:eGFP)i114* line that specifically marks neutrophils with EGFP [21] was used to
145 analyze the fate of intracellular *S. aureus* throughout infection. Imaging throughout whole
146 organisms demonstrated a marked reduction in the number of bacterial cells within individual
147 neutrophils, and that the number of neutrophils containing *S. aureus*, between 2 and 24 h
148 post-infection (**Fig. 1A and 1B**). This result suggested to us that neutrophils could degrade
149 intracellular *S. aureus* effectively throughout infection. Indeed, video timelapse of
150 *Tg(mpx:eGFP)i114* larvae infected with mCherry *S. aureus* demonstrated that bacteria could
151 be effectively degraded by the host neutrophils (**Fig. 1C**), although in other cases the
152 bacterial infection is not controlled (**Fig. S1A**).

153

154 We next sought to determine the location of bacteria and their association with the
155 autophagic machinery within neutrophils. To do this, we used fluorescently tagged Lc3, as
156 has been demonstrated previously in zebrafish and other models [22–24]. We used a newly
157 generated *Tg(lyz:RFP-GFP-lc3)sh383* [24], a double fusion of RFP and GFP, both linked to
158 Lc3, allowing visualization of Lc3 within neutrophils. We first confirmed that in the caudal
159 hematopoietic tissue (CHT), the infection dynamics were similar to the *Tg(mpx:eGFP)i114*
line, with a significant reduction in intracellular bacteria by 26 hpi, indicating bacteria are

160 efficiently controlled and a significant reduction in infected neutrophils was observed (**Fig.**
161 **1D**). Importantly, the number of neutrophils analyzed in the CHT, used for analyses
162 throughout this study, did not significantly change between 2 dpf and 3 dpf (**Fig. S1B**),
163 demonstrating that the change in proportions of infected neutrophils is not due to a large
164 increase in neutrophil number between these time points. The labeling of *S. aureus*-
165 containing vesicles enabled the identification of intracellular bacteria that were within a
166 vesicle (**Fig. 1E**) or free in the cytosol (**Fig. 1F**), as well as non-labeled vesicles, or vesicles
167 marked with Lc3 puncta (**Fig. S1C and S1D**). We found that the proportion of bacteria within
168 vesicles was significantly reduced over time post-injection, whereas the number of bacteria
169 within the cytosol remains relatively constant at a low level, despite becoming proportionally
170 higher relative to vesicular bacteria (**Fig. 1G**). Thus, *S. aureus* phagocytosed by a neutrophil
171 are initially located in a phagocytic vesicle and are subsequently degraded. However, a
172 smaller proportion of *S. aureus* could survive to later infection time points, and these
173 predominantly resided in the cytosol.

174

175 **Generation and characterisation of an in vivo neutrophil GFP-Sqstm1 reporter line.**

176

177 A previous study identified the co-localization of Sqstm1 with *S. aureus* in non-immune cells
178 [18]. Our findings demonstrated a small but significant population of bacteria that were
179 cytosolic, and therefore a possible target for Sqstm1 binding. Accordingly, we generated a
180 transgenic neutrophil-specific Sqstm1 reporter zebrafish line to examine whether Sqstm1
181 and intracellular pathogens are co-localized *in vivo*. We used GFP fused via a small linker
182 region to the N-terminus of *sqstm1* in order to produce a fluorescently marked fusion protein
183 expressed within neutrophils via the *lyz* (lysozyme) promoter [25]. Using larvae with double-
184 labeled neutrophils, we were able to identify GFP-expressing cells from the *Tg(lyz:eGFP-*
185 *sqstm1)**i330* reporter line (hereafter called GFP-Sqstm1 reporter) also expressing mCherry
186 (*Tg(lyz:nfsB-mCherry)**sh260*) [26] in 98% of neutrophils observed (**Fig. S2A-C**).

187 We next examined whether the GFP-Sqstm1 protein is able to function as expected.
188 Interestingly, in the double-labeled larvae, GFP puncta but not mCherry puncta were seen
189 (**Fig. S2D**). Similar Sqstm1 puncta that required ubiquitin-binding domain (UBD) to function
190 have been observed *in vitro* for endogenous Sqstm1 [27]. To test whether the GFP-Sqstm1
191 puncta observed in the GFP-Sqstm1 reporter line respond as expected, GFP-Sqstm1
192 reporter larvae were treated with autophagy inhibitor Bay K8644: known to block autophagy
193 in zebrafish [29]. As expected, there was a significant increase in the number of neutrophils
194 which contained GFP-Sqstm1 puncta following Bay K8644 treatment in comparison to non-
195 treated controls (**Fig. S2E**), as well as a significant increase in the number of GFP-Sqstm1
196 puncta within individual neutrophils as expected for endogenous Sqstm1 (**Fig. S2F**). This

197 result suggests that the GFP-Sqstm1 puncta are not being processed through autophagy
198 and accumulate within the cell, as reported for endogenous Sqstm1 [29]. As we had done for
199 neutrophils and Lc3-positive vesicles, we examined the location of *S. aureus* throughout
200 infection with our GFP-Sqstm1 reporter for consistency with *Tg(mpx:eGFP)i114* and
201 *Tg(lyz:RFP-GFP-Ic3)sh383* (**Fig. 1**). We found that there was a comparable reduction in the
202 number of bacteria observed within neutrophils at 26 hpi in comparison to 2 hpi (**Fig. S3A**)
203 and a reduction in the number of infected neutrophils from 2 hpi to 26 hpi (**Fig. S3B**). This
204 result suggested that neutrophils were efficiently degrading these bacteria, in agreement
205 with **Fig. 1**.

206 Cytosolic bacteria are a possible target for Sqstm1 and *S. aureus* has previously
207 been visualized within the cytosol of a neutrophil from murine infection studies [30]. To
208 identify *S. aureus* in the cytosol in our *in vivo* experiments in zebrafish, we looked for regions
209 of the cytosol that co-localized with *S. aureus* but without a reduction of GFP signal,
210 indicating a vacuole excluding the surrounding cytosol (containing GFP). We first confirmed
211 that we could clearly observe phagosomes containing bacteria with low GFP fluorescence
212 consistent with *S. aureus*-containing vacuoles, where host cell cytoplasm containing GFP,
213 was excluded (Sqstm1GFP^{low}, **Fig. S3C**). As further evidence for this analysis, we
214 determined that vesicles containing *S. aureus*, visualized by TEM, were empty of cellular
215 components, in comparison to the cytosol (**Fig. S3D**), suggesting GFP^{low} areas represent
216 vesicles. Finally, we looked for functional differences consistent with the presence of a
217 phagosomal membrane in GFP^{low} regions by examining pH differences using the pH-
218 sensitive dye pHrodo. We found examples of low pH in vesicles correlating with low
219 cytoplasmic fluorescence (**Fig. S3E**), again suggesting GFP^{low} areas represent vesicles.
220 Having characterized features consistent with an *S. aureus*-containing vacuoles, we were
221 able to assign a subset of bacteria as being in either a damaged phagosome or located in
222 the cytosol (Sqstm1GFP^{high}, **Fig. S3F**). For the purpose of this study, we are defining these
223 bacteria as cytosolic, as they are accessible to cytosolic proteins. We then assigned the
224 cellular location of *S. aureus* by these features at 2 hpi and 26 hpi. We determined that the
225 proportion of *S. aureus* within vesicles was significantly reduced by 26 hpi (**Fig. S3G**) and
226 that the number of bacteria within the cytosol is similar at both time points, in agreement with
227 our *Tg(lyz:RFP-GFP-Ic3)sh383* data (**Fig. 1**).

228

229 ***Lc3 and Sqstm1 are recruited to Staphylococcus aureus within neutrophils.***

230

231 We determined that GFP-Sqstm1 puncta co-localize with *S. aureus* either marking a vesicle
232 containing *S. aureus* (**Fig. 2A and Video S1**) or directly in contact with *S. aureus* located in
233 the cytosol (**Fig. 2B and Video S2**). For puncta marking *S. aureus* in vesicles, no difference

234 in the proportion of vesicles marked was observed at 2 or 26 hpi, although the actual number
235 of puncta-marking vesicles was dramatically reduced by 26 hpi (**Fig. 2C**) as most bacteria
236 had already been degraded. GFP-puncta-marking bacteria in the cytosol were decreased at
237 26 hpi (**Fig. 2D**), as expected, given that Sqstm1 is degraded with the cargo targeted for
238 degradation [29]. We previously showed cytosolic GFP-Sqstm1 puncta were modulated by
239 autophagy machinery-targeting drugs (**Fig. S2E and S2F**). In further agreement with this,
240 comparison between infected and uninfected neutrophils showed there was no difference in
241 the number of cytoplasmic GFP-Sqstm1 puncta at 2 hpi but a significant reduction by 26 hpi
242 (**Fig. 2E and 2F**), indicating these puncta are modulated by *S. aureus* infection.

243 We next examined whether Lc3 can localize to vesicular and cytosolic *S. aureus*. At
244 2 hpi and 26 hpi, there was no difference in the proportion of vesicles marked by Lc3, but
245 most vesicular bacteria are degraded by 26 hpi (**Fig. 2G**), showing that a rapid Lc3 response
246 to *S. aureus* infection occurs. In contrast, vesicles containing *S. aureus* are significantly
247 more likely to have Lc3 puncta associated at 2 hpi (**Fig. 2H and S1D**). However, most
248 bacteria are still cleared by 26 hpi, and there was no significant change in the association of
249 Lc3 puncta to *S. aureus* in the cytosol over time (**Fig. 2I**).

250

251 ***Loss of Sqstm1 reduces zebrafish survival following S. aureus infection.***

252

253 We had demonstrated the steps of Lc3 and the autophagy receptor Sqstm1 recruitment *in*
254 *vivo* in the degradation of *S. aureus* by neutrophils, suggesting a function for Sqstm1 in
255 immunity to *S. aureus* infection by targeting the degradation of bacteria that escaped the
256 phagosome. To test this prediction, we examined the role of Sqstm1 in *S. aureus* zebrafish
257 infection using a morpholino-modified antisense oligonucleotide (morpholino) targeting
258 *sqstm1* [31] to knockdown *sqstm1* expression in the zebrafish larvae. Knockdown of *sqstm1*
259 resulted in a significant reduction in zebrafish survival following *S. aureus* infection,
260 compared to control larvae, supporting a requirement for *sqstm1* in the control of *S. aureus*
261 infection (**Fig. 3A**). Knockdown of *sqstm1* did not reduce larval survival for heat-killed *S.*
262 *aureus* or the non-virulent but closely related bacterium *Micrococcus luteus* (**Fig. S3I and**
263 **S3J**), suggesting Sqstm1 is important for restriction of pathogenic bacteria that escape the
264 phagosome. To further support this conclusion, we generated an *sqstm1* mutant zebrafish
265 (sh558) that lacked a functional UBD domain in *sqstm1*, inhibiting the ability of Sqstm1 to
266 bind to ubiquitinated cargo (**Fig. 3C**). In agreement with our knockdown study, the *sqstm1*
267 mutant zebrafish (sh558) larvae were significantly more susceptible to *S. aureus* infection
268 than wild-type control zebrafish (**Fig. 3B**). Thus, in addition to demonstrating how Lc3 and
269 Sqstm1 were localized during intracellular handling of *S. aureus* by neutrophils, we could
270 independently show the requirement of Sqstm1 in the outcome of infection.

271

272 Both *sqstm1* morpholino and *sqstm1* mutant zebrafish (sh558) techniques do not
273 block Sqstm1 function in neutrophils specifically; therefore, we next aimed to determine
274 whether the loss of Sqstm1 was important in neutrophils during *S. aureus* infection.
275 Interestingly, there was no difference between the survival of our GFP-Sqstm1 reporter and
276 wild-type controls (**Fig. S3H**), suggesting that endogenous *sqstm1* expression is sufficient
277 for restriction of the small proportion of bacteria which reside in the cytosol. First, using
278 tyramide signal amplification (TSA) staining of 1 dpi larvae to visualize neutrophils within
279 *sqstm1* mutant (sh558) and control larvae, we found a non-significant ($p=0.1039$) increase in
280 neutrophils containing *S. aureus* (**Fig. 3D**). A small effect was expected due to the small
281 proportion of cytosolic bacteria, which are likely targeted by Sqstm1 during infection. It was,
282 therefore, likely that showing a difference in the number of infected neutrophils would have
283 required a very large number of infections. We were able to calculate that the observed
284 differences would require a group size of 270.

285 Next, using *sqstm1* morphants and control larvae, a comparison of the number of
286 bacteria present within neutrophils at 1 dpi was completed in the *Tg(mpx:eGFP)i114* larvae.
287 In agreement with the Sqstm1-UBD mutant data, a non-significant ($p=0.115$) increase of
288 neutrophils containing *S. aureus* was observed in *sqstm1* morphants in comparison to wild-
289 type controls (**Fig. 3E**). Again, we had calculated that the observed differences would require
290 a large group size of 219. However, the examination of the bacterial location revealed a
291 significant increase in the number of cytosolic *S. aureus* in the *sqstm1* morphants in
292 comparison to control fish (**Fig. 3F**), suggesting loss of Sqstm1 is important for the control of
293 cytosolic *S. aureus* by neutrophils. Thus, we could show that loss of *sqstm1* leads to an
294 increase in bacterial burden within neutrophils and that Sqstm1 is likely targeting the small
295 proportion of bacteria that escape to the cytosol.

296

297 **Discussion**

298 Using the unique attributes of long-term high-resolution imaging and genetic manipulation of
299 zebrafish larvae, we have shown the dynamics of Lc3 and Sqstm1 on the *S. aureus*-
300 containing vacuoles, their relation to bacterial degradation, and how Sqstm1 recognizes
301 cytosolic bacteria, meaning that loss of Sqstm1 activity is sufficient to increase mortality
302 following *S. aureus* infection.

303 Loss of zebrafish *sqstm1*, through morpholino-mediated knockdown, significantly
304 increased susceptibility to the infection to *S. aureus*. This result is the first *in vivo* evidence
305 that Sqstm1 is important in the outcome of intracellular handling of *S. aureus*. To confirm the
306 *sqstm1* knockdown data, we generated a zebrafish *sqstm1* mutant lacking the UBD domain,
307 which confirmed a significant increase in the susceptibility of zebrafish to *S. aureus* infection.
308 This result suggests that for *S. aureus* infection control, the Sqstm1 UBD, which can bind to

309 ubiquitinated *S. aureus* [18,20], is important for host control of infection. In addition to its role
310 as an autophagy receptor, Sqstm1 can aid in the killing of pathogens through the delivery of
311 anti-microbial peptides [32]. Thus, it is possible that anti-microbial peptides delivered by
312 Sqstm1 are important in neutrophil control of *S. aureus* infection. The *sqstm1* zebrafish
313 mutant represents a valuable tool in the analysis of selective autophagy in infection, which
314 may also be useful for the study of other intracellular pathogens or in other diseases, where
315 autophagy is implicated in pathology, for example in neurodegenerative disorders.

316 Although *in vitro* studies have described co-localization of Sqstm1 and autophagy in
317 pathogen handling, until now, no evidence of direct Sqstm1 interactions with these
318 pathogens has been shown in neutrophils or *in vivo*. Interaction of Sqstm1 with *S. aureus*
319 has been demonstrated through *in vitro* studies using fibroblasts and epithelial cells [18,20].
320 *In vitro* data shows *S. aureus* can be targeted for autophagic degradation by Sqstm1 [18,20],
321 where puncta appear to be co-localized with *S. aureus*. Our new zebrafish GFP-Sqstm1
322 reporter shows cytosolic puncta formation, which has also been observed in other cell
323 culture studies, both endogenous expression and using similar GFP-Sqstm1 reporter
324 systems [27,33,34]. By comparing GFP-Sqstm1 puncta marking of intracellular *S. aureus*
325 with the location of bacteria over time, it is interesting to note that Sqstm1 marking is
326 reduced over time for cytosolic bacteria, which appear to be a small population that persists
327 throughout infection. This result may indicate that cytosolic bacteria marked with Sqstm1 are
328 degraded. Furthermore, at later time points in *S. aureus* infection, the number of GFP-
329 Sqstm1 puncta is reduced within infected cells, suggesting that when bacteria escape the
330 phagosome, Sqstm1 becomes important in controlling cytosolic bacteria.

331 We show that most *S. aureus* is contained within a vesicle soon after infection, and
332 by 26 hpi, most *S. aureus* are absent from neutrophils. Of note, some images show bacteria
333 outside the neutrophils that have been phagocytosed by macrophages, which has previously
334 been described [35]. The large reduction of neutrophils containing bacteria from 2 hpi to 26
335 hpi, leaving a small population at 26 hpi, may be representative of a niche for bacterial
336 persistence and/or proliferation. The role of neutrophils as an intracellular niche has
337 previously been described to be important in determining the outcome of *S. aureus* infection
338 [15,16,36]. Interestingly, it appears that Lc3 marks the majority of vesicles containing
339 bacteria. Lc3 localization to *S. aureus* may represent Lc3 recruitment to autophagosomes;
340 however, since recruitment is observed at early infection time points, it may represent Lc3-
341 associated phagocytosis, which is also observed in *Listeria monocytogenes* infection of
342 macrophages [37]. Since most bacteria are degraded, it appears that Lc3 marking of
343 vesicles could lead to bacterial degradation in the zebrafish.

344 Thus, we demonstrate that host Sqstm1 is beneficial for the host outcome following
345 *S. aureus* infection and that Sqstm1-mediated control of cytosolic bacteria within neutrophils

346 may represent one of many mechanisms employed by the host in immunity to this versatile
347 pathogen.

348

349

350

351

352 **Materials and methods**

353

354 ***Ethics statement.***

355

356 Animal work was carried out according to guidelines and legislation set out in UK law in
357 the Animals (Scientific Procedures) Act 1986, under Project License PPL 40/3574 or
358 P1A4A7A5E). Ethical approval was granted by the University of Sheffield Local Ethical
359 Review Panel. Animal work completed in Singapore was completed under the Institutional
360 Animal Care and Use Committee (IACUC) guidelines under the A*STAR Biological
361 Resource Centre (BRC) approved IACUC Protocol #140977.

362

363 ***Zebrafish husbandry.***

364

365 Zebrafish strains were maintained according to standard protocols [38]. For animals
366 housed in the Bateson Centre aquaria at the University of Sheffield, adult fish were
367 maintained on a 14:10-h light/dark cycle at 28°C in UK Home Office approved facilities.
368 For animals housed in IMCB, Singapore, adult fish were maintained on a 14:10-h
369 light/dark cycle at 28°C in the IMCB zebrafish facility. London wild-type (LWT) and AB wild-
370 type larvae were used in addition to transgenic lines, *Tg(lyz:eGFP-sqstm1)i330* created in
371 this study, *Tg(lyz:RFP-GFP-Lc3)sh383* [24], *Tg(lyz:nfsB-mCherry)sh260* [26] (these fish
372 encode nitroreductase gene *nfsB* within neutrophils which allows ablation of cells following
373 metronidazole treatment, which was not used in this study) and *Tg(mpx:eGFP)i114* [21].
374 Generation of *Sqstm1* sh558 mutant zebrafish is described below. Larvae were maintained
375 in E3 (5 mM NaCl, 0.17 mM KCl, 0.33 mM CaCl₂, 0.33 mM MgSO₄) plus methylene blue
376 (Sigma-Aldrich, 50484) at 28°C until 5 dpf.

377

378 ***S. aureus culture.***

379

380 The *Staphylococcus aureus* strain SH1000 [39] was used in this study. A single bacterial
381 colony was placed in 10 ml brain heart infusion medium (Thermo Fisher Scientific,
382 OxoidCM1135B) overnight at 37°C, 250 rpm. 500 µl of this overnight culture was then added
383 to 50 ml of brain heart infusion medium and incubated at 37°C, 250 rpm until OD₆₀₀ 1. The
384 bacteria were then pelleted at 5445 x g, 4°C for 15 min. The bacteria were then
385 resuspended in PBS (Oxoid, BR0014G), using a volume to dilute to the required dose, with
386 1500 colony-forming units (cfu)/nL being standard. Bacteria were incubated on ice for a short
387 period, until use. Strains used: SH1000 wild-type strain [39], SH1000-pMV158-mCherry [40],
388 SH1000-pMV158-GFP [40].

389

390 ***Zebrafish micro-injection.***

391

392 For *sqstm1* morpholino microinjections: Larvae were injected immediately after
393 fertilization using an *sqstm1* morpholino [31]. A standard control morpholino (Genetools)
394 was used as a negative control. For injection of *S. aureus*, zebrafish larvae were injected
395 at 1 dpf (for survival analysis, [36]) or 2 dpf (for microscopy analysis) and monitored until
396 a maximum of 5 dpf. Larvae were anesthetized by immersion in 0.168 mg/mL tricaine
397 (Pharmaq Ltd, ATC QN01AX93) in E3 and transferred onto 3% methyl cellulose (Sigma-
398 Aldrich, M0387) in E3 for injection. For *S. aureus* 1 nl of bacteria, containing 1500 cfu,
399 was injected into the yolk sac circulation valley. Larvae were transferred to fresh E3 to
400 recover from anesthetic. Any zebrafish injured by the needle/micro-injection were
401 removed from the procedure. Zebrafish were maintained at 28°C.

402

403 ***Generation of Tg(lyz:eGFP-sqstm1)i330 transgenic line.***

404

405 The generation of the *Tg(lyz:eGFP-sqstm1)i330* line was performed using the Gateway™
406 system in combination with Tol2 transgenesis [41]. To make the required expression clone,
407 *pDest(lyz:eGFP-sqstm1)*, the *p5E-lyz* entry clone [42] and the *pME-eGFP-nostop* [41] middle
408 entry vectors were used. The destination vector *pDesttol2CG* [41], was chosen, which
409 included *tol2* sites for integration into the genome, in addition to a GFP heart marker. The
410 required *sqstm1* 3' entry vector and expression clone *pDest(lyz:eGFP-sqstm1)* were
411 constructed following the Multisite Gateway™ three-fragment vector construction kit
412 (Invitrogen, 12537-023). To generate *tol2* mRNA, a *pCS2FA-transposase* plasmid [41] was
413 used. The DNA plasmid was linearized through a restriction site digest. *tol2* mRNA was
414 generated by a transcription reaction (Ambion T3 mMessage Machine). *tol2* mRNA and
415 *pDest(lyz:eGFP-sqstm1)* were co-injected into a single cell (at the single cell stage) of wild-
416 type AB larvae. A 1 nl injection contained 30 pg of *tol2* mRNA and 60 pg of *pDest(lyz:eGFP-*
417 *sqstm1)*.

418

419 ***Microscopy of infected zebrafish.***

420

421 Larvae were anesthetized 0.168 mg/mL tricaine in E3 and mounted in 0.8% low melting
422 agarose (Affymetrix, 32830) onto glass-bottom microwell dishes (MatTek, P35G-1.5-14C).
423 An UltraVIEW VoX spinning disk confocal microscope (Perkin Elmer, Cambridge, UK) was
424 used for imaging neutrophils within larvae. 405-nm, 445-nm, 488-nm, 514-nm, 561-nm and
425 640-nm lasers were available for excitation. Most cellular level imaging was completed in the

426 caudal hematopoietic tissue (CHT) using a 40x oil objective (UplanSApo 40x oil [NA 1.3]). In
427 some cases, a 20x objective was used for whole larvae imaging. GFP, TxRed emission
428 filters were used and bright-field images were acquired using a Hamamatsu C9100-50 EM-
429 CCD camera. Volocity software was used. Between early and late time points, zebrafish
430 larvae were placed back into E3 and maintained at 28°C.

431

432 ***pHrodo staining of S. aureus.***

433

434 Bacterial strains were prepared for injected (as above) and resuspended into PBS pH 9.
435 pHrodo (Thermo Fisher Scientific, P36600) was added at a ratio of 1:200 and incubated
436 at 37°C for 30 min, shaking, in the dark. The bacteria were suspended in PBS pH 8 and
437 washed through a series of solutions (Tris, pH 8.5, PBS pH 8) and finally resuspended
438 into PBS pH 7.4 for injection.

439

440 ***Tyramide Signal Amplification (TSA) Staining.***

441

442 Following *S. aureus* infection, larvae were fixed in paraformaldehyde (Thermo Fisher
443 Scientific, 28908) diluted to 4% in PBS, overnight at 4°C. Once fixed, larvae were washed
444 in PBS thrice. Staining of neutrophils (specifically myeloperoxidase activity) in LWT larvae
445 was completed using TSA staining kit (Cy5-TSA Cyanine Kit; PerkinElmer,
446 NEL705A001KT). Fish were incubated in a 1:100 ratio of Cy5-TSA:amplification diluent at
447 28°C for 10 min in the dark. Larvae were washed thrice in PBS before imaging.

448

449 ***TEM of infected zebrafish.***

450

451 Specimens were fixed in 2.5% glutaraldehyde (Agar Scientific, AGR1010), in 0.1 M sodium
452 cacodylate (Agar Scientific, AGR1105) and post-fixed 2% aqueous osmium tetroxide,
453 dehydrated through graded series of ethanol, and cleared in propylene oxide (Agar
454 Scientific, AGR1080) and then infiltrated in 50:50 Araldite resin (Araldite resin made up of a
455 50:50 dodecanyl succinic anhydride (Agar Scientific, AGR1051) and Araldite resin
456 CY212 (Agar Scientific, AGR1040) mix plus 1 drop/ml benzyl dimethylamine (Agar Scientific,
457 AGR1060) and propylene oxide (Agar Scientific, AGR1080) mixture overnight on a rotor.
458 This mixture was replaced with two changes over 8 h of fresh Araldite resin mixture before
459 being embedded in fresh resin and cured in a 60°C oven for 48-72 h. Ultrathin sections,
460 approximately 85-nm thick, were cut on a Leica UC6 ultramicrotome onto 200-mesh copper
461 grids (Agar Scientific, G2200C). These were stained for 10 min with saturated aqueous
462 uranyl acetate followed by Reynolds lead citrate [43] for 5 min. Sections were examined

463 using a FEI Tecnai Transmission Electron Microscope at an accelerating voltage of 80
464 kV. Electron micrographs were recorded using Gatan Orius 1000 digital camera and Gatan
465 Digital Micrograph software.

466

467 ***Image analysis.***

468

469 Image analysis was performed using ImageJ software [44] to quantify the number of *S.*
470 *aureus* cells within neutrophils and to quantify GFP-Sqstm1 puncta and Lc3 co-
471 localization to these pathogens.

472

473 ***Drug treatment of zebrafish.***

474

475 Larvae were treated with an autophagy inhibitor through immersion in E3 medium. Bay
476 K8644 (Sigma-Aldrich, B2112) was added to the E3 to the required concentration of 1 μ M.
477 Larvae were incubated at 28°C for 24 h before microscopy. Zebrafish were not anesthetized
478 for immersion drug treatments.

479

480 ***Generation of sqstm1 mutant.***

481

482 A zebrafish *sqstm1* mutant was generated using CRISPR-Cas9 mutagenesis. A guide RNA
483 targeting exon 8 of zebrafish *sqstm1* (ACAGAGACTCCACCAGCCTA) was inserted into a
484 published oligonucleotide scaffold [45] and injected together with recombinant Cas9 protein
485 (New England Biolabs) into 1-2 cell stage zebrafish (AB strain). Efficiency of mutagenesis
486 was confirmed using high-resolution melt curve analysis as previously described [46] and
487 several founders were identified. *sqstm1*^{sh558} carries a 10-base pair deletion resulting in a
488 frameshift and premature truncation of Sqstm1 in the ubiquitin-associated (UBA) domain.

489

490 ***Statistical analysis.***

491

492 Statistical analysis was performed as described in the results and figure legends. We
493 used Graph Pad Prism 7 (v7.04) for statistical tests and plots. Fisher's exact tests, which
494 are reliable with very small group sizes, were used to analyze data sets that have uneven
495 group sizes. In these cases, small group sizes were unavoidable due to the nature of
496 these experiments in which we describe only a very small proportion of bacterial cells are
497 observed at later time points in zebrafish infection.

498

499 **Acknowledgments**

500 JFG was supported by an award from the Singapore A*STAR Research Attachment
501 Programme (ARAP) in partnership with the University of Sheffield, and a Medical Research
502 Council Grant (MR/R001111/1 with SAR and SJF). TKP was supported by an individual
503 Marie Curie fellowship (PIEF-GA-2013-625975) and by AMR cross-council funding from the
504 MRC to the SHIELD consortium “Optimising Innate Host Defence to Combat Antimicrobial
505 Resistance” MRNO2995X/1. RDT and AJG were supported by the University of Sheffield.
506 JJS was a Marie Curie fellow in the Initial Training Network FishForPharma (PITN-GA-2011-
507 289209). Work in the PWI lab was funded by the A*STAR Institute of Molecular and Cell
508 Biology (IMCB) and the Lee Kong Chian School of Medicine. SAJ was supported by the
509 Medical Research Council and Department for International Development Career
510 Development Award Fellowship MR/J009156/1 (<http://www.mrc.ac.uk/>). SAJ was additionally
511 supported by a Krebs Institute Fellowship (<http://krebsinstitute.group.shef.ac.uk/>), and
512 Medical Research Council Centre grant (G0700091). SAR was supported by a Medical
513 Research Council Programme Grant (MR/M004864/1) (<http://www.mrc.ac.uk/>). Imaging was
514 completed at the Wolfson Light Microscopy Facility. We thank the aquarium staff at the
515 Bateson Centre (Sheffield) and the IMCB (Singapore) for zebrafish husbandry.

516

517 **Declaration of interest statement**

518 The authors have no conflict of interests

519

520

521 **References**

- 522 1. Mizushima N, Levine B, Cuervo A, Klionsky D. Autophagy fights disease through
523 cellular self-digestion. *Nature*. 2008;451(7182):1069–75.
- 524 2. Tanida I. Autophagy basics. *Microbiol Immunol*. 2011 Jan;55(1):1–11.
- 525 3. Gatica D, Lahiri V, Klionsky DJ. Cargo recognition and degradation by selective
526 autophagy. *Nat Cell Biol*. 2018 Mar;20(3):233–42.
- 527 4. Sharma V, Verma S, Seranova E, Sarkar S, Kumar D. Selective Autophagy and
528 Xenophagy in Infection and Disease. *Front cell Dev Biol*. 2018;6:147.
- 529 5. Popovic D, Dikic I. The molecular basis of selective autophagy. *Biochem (Lond)*.
530 2012;34(2):24–30.
- 531 6. Rogov V, Dötsch V, Johansen T, Kirkin V. Interactions between autophagy receptors
532 and ubiquitin-like proteins form the molecular basis for selective autophagy. *Mol Cell*.
533 2014 Jan;53(2):167–78.
- 534 7. Farré J-C, Subramani S. Mechanistic insights into selective autophagy pathways:
535 lessons from yeast. *Nat Rev Mol Cell Biol*. 2016 Jul 6;17(9):537–52.
- 536 8. Levine B, Mizushima N, Virgin H. Autophagy in immunity and inflammation. *Nature*.
537 2011;469(7330):323–35.
- 538 9. Zhang R, Varela M, Vallentgoed W, Forn-Cuni G, van der Vaart M, Meijer AH. The
539 selective autophagy receptors Optineurin and p62 are both required for zebrafish host
540 resistance to mycobacterial infection. Behr MA, editor. *PLOS Pathog*. 2019 Feb
541 28;15(2):e1007329.
- 542 10. Mostowy S, Sancho-Shimizu V, Hamon MA, Simeone R, Brosch R, Johansen T, et al.
543 p62 and NDP52 proteins target intracytosolic *Shigella* and *Listeria* to different
544 autophagy pathways. *J Biol Chem*. 2011 Jul 29;286(30):26987–95.
- 545 11. Deretic V, Levine B. Autophagy, immunity, and microbial adaptations. *Cell Host*
546 *Microbe*. 2009;5(6):527–49.
- 547 12. Amer AO, Swanson MS. Autophagy is an immediate macrophage response to
548 *Legionella pneumophila*. *Cell Microbiol*. 2005 Jun;7(6):765–78.
- 549 13. Hernandez LD, Pypaert M, Flavell R a, Galán JE. A *Salmonella* protein causes
550 macrophage cell death by inducing autophagy. *J Cell Biol*. 2003 Dec 8;163(5):1123–
551 31.
- 552 14. Gutierrez MG, Vázquez CL, Munafó DB, Zoppino FCM, Berón W, Rabinovitch M, et
553 al. Autophagy induction favours the generation and maturation of the *Coxiella*-
554 replicative vacuoles. *Cell Microbiol*. 2005 May 12;7(7):981–93.
- 555 15. Thwaites GE, Gant V. Are bloodstream leukocytes Trojan Horses for the metastasis
556 of *Staphylococcus aureus*? *Nat Rev Microbiol*. 2011 Mar 7;9(3):215–22.
- 557 16. Prajsnar TK, Hamilton R, Garcia-Lara J, McVicker G, Williams A, Boots M, et al. A
558 privileged intraphagocyte niche is responsible for disseminated infection of
559 *Staphylococcus aureus* in a zebrafish model. *Cell Microbiol*. 2012 Oct;14(10):1600–
560 19.
- 561 17. Schnaith A, Kashkar H, Leggio SA, Addicks K, Krönke M, Krut O. *Staphylococcus*
562 *aureus* subvert autophagy for induction of caspase-independent host cell death. *J Biol*
563 *Chem*. 2007 Jan 26;282(4):2695–706.
- 564 18. Neumann Y, Bruns SA, Rohde M, Prajsnar TK, Foster SJ, Schmitz I. Intracellular
565 *Staphylococcus aureus* eludes selective autophagy by activating a host cell kinase.
566 *Autophagy*. 2016 Nov 14;12(11):2069–84.
- 567 19. Bayles KW, Wesson CA, Liou LE, Fox LK, Bohach GA, Trumble WR. Intracellular
568 *Staphylococcus aureus* escapes the endosome and induces apoptosis in epithelial
569 cells. *Infect Immun*. 1998 Jan;66(1):336–42.
- 570 20. Singh A, Patel P, Tomar D, Singh R, Sripada L, Prajapati P, et al. TBK1 regulates
571 p62/sqstm1 mediated autophagic clearance of intracellular ubiquitinated
572 *Staphylococcus aureus* in human epithelial cells. *Transl Genet Genomics*.
573 2017;[online fi.
- 574 21. Renshaw SA, Loynes CA, Trushell DMI, Elworthy S, Ingham PW, Whyte MKB. A
575 transgenic zebrafish model of neutrophilic inflammation. *Blood*. 2006;108(13).

- 576 22. Mathai B, Meijer A, Simonsen A. Studying Autophagy in Zebrafish. *Cells*. 2017 Jul
577 9;6(3):21.
- 578 23. Li L, Wang Z V., Hill JA, Lin F. New Autophagy Reporter Mice Reveal Dynamics of
579 Proximal Tubular Autophagy. *J Am Soc Nephrol*. 2014 Feb;25(2):305–15.
- 580 24. Prajsnar TK, Serba JJ, Dekker BM, Gibson JF, Masud S, Fleming A, et al. The
581 autophagic response to *Staphylococcus aureus* provides an intracellular niche in
582 neutrophils. *bioRxiv*. 2019 Mar 18;581223.
- 583 25. Yang C-T, Cambier CJ, Davis JM, Hall CJ, Crosier PS, Ramakrishnan L. Neutrophils
584 exert protection in the early tuberculous granuloma by oxidative killing of
585 mycobacteria phagocytosed from infected macrophages. *Cell Host Microbe*. 2012
586 Sep 13;12(3):301–12.
- 587 26. Buchan KD, Prajsnar TK, Ogryzko N V, Jong NW de, Gent M van, Kolata J, et al. A
588 transgenic zebrafish line for in vivo visualisation of neutrophil myeloperoxidase.
589 *bioRxiv*. 2019 Mar 20;456541.
- 590 27. Bjørkøy G, Lamark T, Brech A, Outzen H, Perander M, Øvervatn A, et al.
591 p62/SQSTM1 forms protein aggregates degraded by autophagy and has a protective
592 effect on huntingtin-induced cell death. *J Cell Biol*. 2005;171(4).
- 593 28. Williams A, Sarkar S, Cuddon P, Ttofi EK, Saiki S, Siddiqi FH, et al. Novel targets for
594 Huntington’s disease in an mTOR-independent autophagy pathway. *Nat Chem Biol*.
595 2008 May;4(5):295–305.
- 596 29. Bjørkøy G, Lamark T, Pankiv S, Øvervatn A, Brech A, Johansen T. Chapter 12
597 Monitoring Autophagic Degradation of p62/SQSTM1. In 2009. p. 181–97.
- 598 30. Gresham HD, Lowrance JH, Caver TE, Wilson BS, Cheung AL, Lindberg FP. Survival
599 of *Staphylococcus aureus* inside neutrophils contributes to infection. *J Immunol*. 2000
600 Apr 1;164(7):3713–22.
- 601 31. van der Vaart M, Korbee CJ, Lamers GEM, Tengeler AC, Hosseini R, Haks MC, et al.
602 The DNA Damage-Regulated Autophagy Modulator DRAM1 Links Mycobacterial
603 Recognition via TLR-MYD88 to Autophagic Defense. *Cell Host Microbe*. 2014 Jun
604 11;15(6):753–67.
- 605 32. Ponpuak M, Davis AS, Roberts EA, Delgado MA, Dinkins C, Zhao Z, et al. Delivery of
606 cytosolic components by autophagic adaptor protein p62 endows autophagosomes
607 with unique antimicrobial properties. *Immunity*. 2010 Mar 26;32(3):329–41.
- 608 33. Larsen KB, Lamark T, Øvervatn A, Harneshaug I, Johansen T, Bjørkøy G. A reporter
609 cell system to monitor autophagy based on p62/SQSTM1. *Autophagy*. 2010;66:784–
610 93.
- 611 34. Pankiv S, Clausen TH, Lamark T, Brech A, Bruun J-A, Outzen H, et al. p62/SQSTM1
612 binds directly to Atg8/LC3 to facilitate degradation of ubiquitinated protein aggregates
613 by autophagy. *J Biol Chem*. 2007 Aug 17;282(33):24131–45.
- 614 35. Prajsnar TK, Cunliffe VT, Foster SJ, Renshaw S a. A novel vertebrate model of
615 *Staphylococcus aureus* infection reveals phagocyte-dependent resistance of zebrafish
616 to non-host specialized pathogens. *Cell Microbiol*. 2008 Nov;10(11):2312–25.
- 617 36. Pollitt EJG, Szkuta PT, Burns N, Foster SJ. *Staphylococcus aureus* infection
618 dynamics. *PLoS Pathog*. 2018;14(6):e1007112.
- 619 37. Gluschko A, Herb M, Wiegmann K, Krut O, Neiss WF, Utermöhlen O, et al. The β 2
620 Integrin Mac-1 Induces Protective LC3-Associated Phagocytosis of *Listeria*
621 *monocytogenes*. *Cell Host Microbe*. 2018 Mar 14;23(3):324-337.e5.
- 622 38. Nüsslein-Volhard C (Christiane), Dahm R. *Zebrafish : a practical approach*. Oxford
623 University Press; 2002.
- 624 39. Horsburgh MJ, Aish JL, White IJ, Shaw L, Lithgow JK, Foster SJ, et al. Omega B
625 Modulates Virulence Determinant Expression and Stress Resistance:
626 Characterization of a Functional rsbU Strain Derived from *Staphylococcus aureus*
627 8325-4. *J Bacteriol*. 2002;184(19):5457–67.
- 628 40. Boldock E, Surewaard BGJ, Shamarina D, Renshaw S, Foster S. Human skin
629 commensals augment *Staphylococcus aureus* pathogenesis. *Nat Microbiol*.
630 2018;3:881–90.

- 631 41. Kwan KM, Fujimoto E, Grabher C, Mangum BD, Hardy ME, Campbell DS, et al. The
632 Tol2kit: A multisite gateway-based construction kit for Tol2 transposon transgenesis
633 constructs. *Dev Dyn*. 2007 Nov;236(11):3088–99.
- 634 42. Elks PM, van Eeden FJ, Dixon G, Wang X, Reyes-Aldasoro CC, Ingham PW, et al.
635 Activation of hypoxia-inducible factor-1 α (Hif-1 α) delays inflammation resolution by
636 reducing neutrophil apoptosis and reverse migration in a zebrafish inflammation
637 model. *Blood*. 2011 Jul 21;118(3):712–22.
- 638 43. Reynolds ES. The use of lead citrate at high pH as an electron-opaque stain in
639 electron microscopy. *J Cell Biol*. 1963 Apr;17(1):208–12.
- 640 44. Rasband WS. ImageJ. U.S. National Institutes of Health, Bethesda, Maryland, USA,
641 <https://imagej.nih.gov/ij/>, 1997-2018.;
- 642 45. Talbot JC, Amacher SL. A streamlined CRISPR pipeline to reliably generate zebrafish
643 frameshifting alleles. *Zebrafish*. 2014 Dec;11(6):583–5.
- 644 46. Sutton BC, Allen RA, Zhao ZJ, Dunn ST. Detection of the JAK2V617F mutation by
645 asymmetric PCR and melt curve analysis. *Cancer Biomarkers*. 2007 Nov
646 16;3(6):315–24.
- 647
648

649 **Figure Legends**

650 **Figure 1.** *Staphylococcus aureus* location within neutrophils changes from vesicular to cytosolic
651 throughout infection. **(A-B)** *Tg(mpx:eGFP)i114* larvae were injected at 1 dpf with 1500 cfu SH1000
652 mCherry *S. aureus*, and imaged at early (1-5 hpi) and late (24-28 hpi) time points. **(A)** Number of
653 bacteria contained in neutrophils, with maximum 100 bacterial cells counted (whole larvae imaged,
654 n=11-13, Mann-Whitney test, ****p<0.0001, +/- SD). **(B)** Proportion of neutrophils containing bacteria
655 (whole larvae imaged, n=11-12, unpaired t-test, ****p<0.0001, +/- SEM) **(C)** *Tg(mpx:eGFP)i114* larvae
656 were injected at 1 dpf with 1500 cfu SH1000 mCherry *S. aureus*, and imaged at 3 h post-infection.
657 Images were captured every 5 min for 12 h at multiple z planes to follow infected neutrophils over
658 time (scale: 5 μ m). **(D-G)** *Tg(lyz:RFP-GFP-lc3)sh383* larvae were injected at 2 dpf with GFP *S.*
659 *aureus*, and imaged in the CHT at 2 hpi, and ~26 hpi. **(D)** The proportion of infected or non-infected
660 neutrophils at 2 hpi and 26 hpi (****p<0.0001 Chi-Square test, n=3, 17 2 hpi larvae, 11 26 hpi larvae).
661 **(E)** *S. aureus* with Lc3 marking the entire vesicle (scale: 9 μ m), demonstrating a vesicle. **(F)** *S. aureus*
662 in the cytosol (scale: 9 μ m). **(G)** Proportion *S. aureus* events observed within vesicles or cytosol at 2
663 hpi and 26 hpi (**p<0.001, Fisher's exact test, n=3, 17 larvae at 2 hpi, and 11 larvae at 26 hpi).
664

665 **Figure 2.** *In vivo* recruitment of GFP-Sqstm1 puncta during *S. aureus* infection. **(A)** Representative
666 image of *S. aureus* observed within a likely "vesicle" with GFP-Sqstm1 puncta localization, (scale: 7
667 μ m) **(B)** representative image of *S. aureus* observed within the cytosol with GFP-Sqstm1 puncta
668 localization, (scale: 9 μ m) **(C)** *S. aureus* within vesicles, co-localized with GFP-Sqstm1 at 2 hpi and 26
669 hpi (CHT imaged, ns, Fisher's exact test, n=3, 14 larvae at 2 hpi, and 12 larvae at 26 hpi) **(D)** *S.*
670 *aureus* in the cytosol, co-localized with GFP-Sqstm1 at 2 hpi and 26 hpi (CHT imaged, *p<0.05,
671 Fisher's exact test, n=3, 14 larvae at 2 hpi, and 12 larvae at 26 hpi) **(E)** GFP-Sqstm1 puncta in the
672 cytosol of infected and non-infected at 2 hpi (CHT imaged, ns, Mann-Whitney test, n=3, error bars +/-
673 SD, 14 larvae) **(F)** GFP-Sqstm1 puncta in the cytosol of infected and non-infected at 26 hpi (CHT
674 imaged, **p<0.01, Mann-Whitney test, n=3, error bars +/- SD, 12 larvae) **(G-I)** 2500 cfu of GFP *S.*
675 *aureus* injected into *Tg(lyzC:RFP-GFP-lc3)sh383*, larvae imaged in the CHT at 2 hpi and 26 hpi. **(G)**
676 Lc3 association to the entire *S. aureus* vesicle at 2 hpi and 26 hpi (ns, Fisher's test, n =3, 17 2 hpi
677 larvae, 11 26 hpi larvae) **(H)** The number of *S. aureus* vesicles with Lc3 puncta (*p<0.05, Fisher's test,
678 n =3, 17 2 hpi larvae, 11 26 hpi larvae) **(I)** The number of *S. aureus* events in the cytosol with Lc3
679 puncta at 2 hpi and 26 hpi (ns, Fisher's test, n =3, 17 larvae at 2 hpi, 11 larvae at 26 hpi).
680

681 **Figure 3.** Zebrafish survival is reduced following infection with *Staphylococcus aureus* in the absence
682 of Sqstm1. **(A-B)** Zebrafish survival following *S. aureus* infection, larvae were injected with 1500 cfu of
683 SH1000 at 30 hpf. **(A)** *sqstm1* morphants or control morphants survival (n=3, 74-80 larvae per group,
684 p=0.004, Log-rank, Mantel-Cox test) **(B)** *sqstm1* mutant or wild-type sibling survival (n=3, 57-60
685 larvae per group, p=0.0168, Log-rank, Mantel-Cox test) **(C)** Electropherograms showing the sequence
686 of wild type and sh558 mutant Sqstm1. Dashed vertical lines show the location of the 5-bp deletion.
687 The position of the frameshift in the Sqstm1 protein is illustrated. Since this frameshift is located in the
688 final coding exon, we predict translation of a truncated Sqstm1 protein lacking the UBD domain. **(D-E)**
689 Number of infected neutrophils at 26 hpi following *S. aureus* infection, larvae were injected with 1500
690 cfu of SH1000 mCherry (D) or GFP (E), imaging completed in CHT at 30 hpf **(D)** *sqstm1* mutant or
691 wild-type sibling (n=3, 19-36 larvae per group, p=0.0168, p=0.1039, Mann-Whitney test, error bars +/-
692 SEM) **(E)** *sqstm1* morphants or control morphants in *Tg(mpx:eGFP)i114* larvae (n=3, 32-34 larvae per
693 group, p=0.115, Mann-Whitney test, error bars +/- SEM) **(F)** Number of neutrophils containing
694 cytosolic *S. aureus* in *sqstm1* morphants or control morphants *Tg(mpx:eGFP)i114* larvae (n=3, 32-34
695 larvae per group, **p<0.01, Mann-Whitney test, error bars +/- SEM)

Figure 1

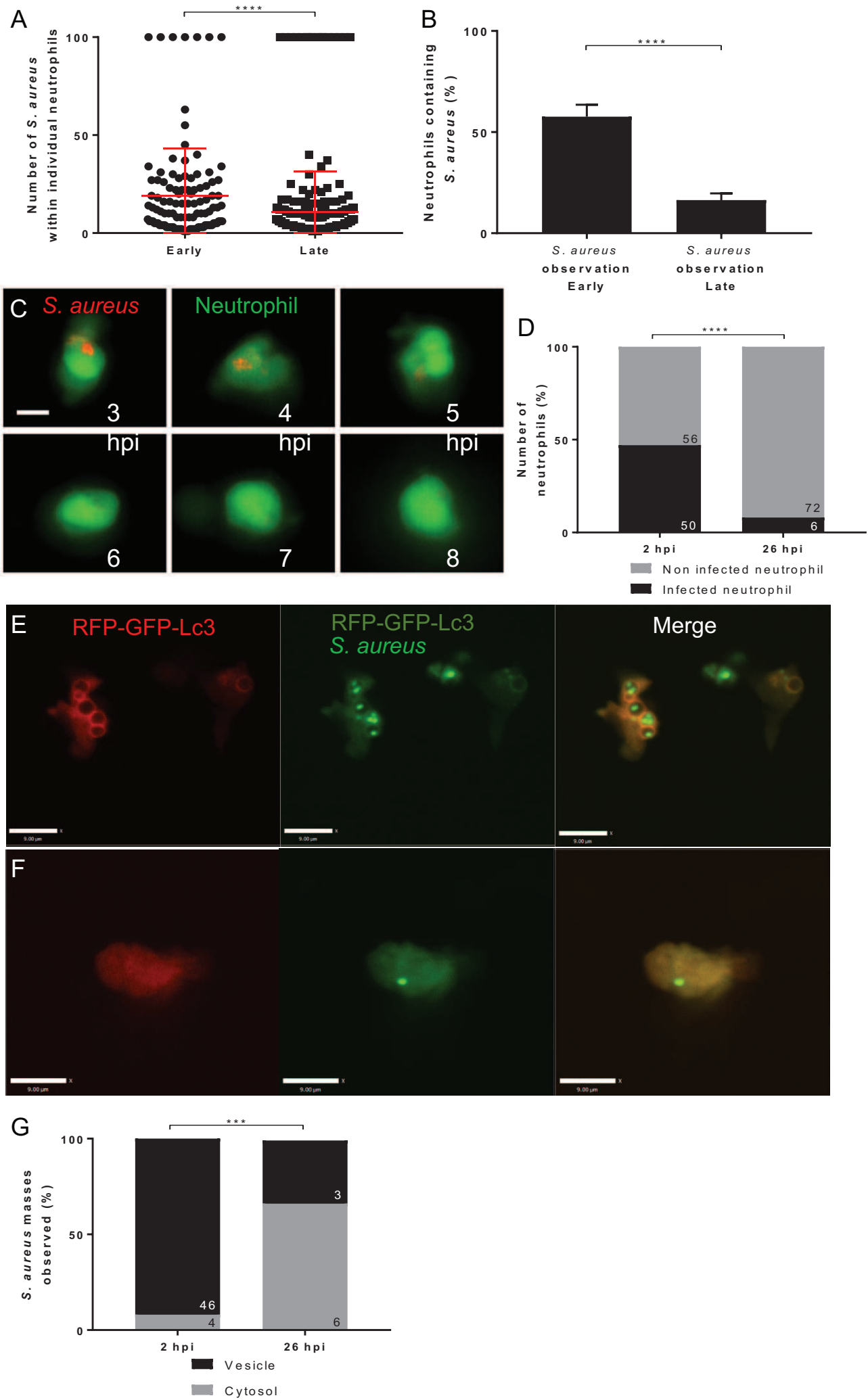


Figure 3

